

Electronic Supplementary Information for

Hierarchically Porous SiC Ultrathin Fibers Mat with Enhanced Mass Transport, Amphipathic Property and High-Temperature Erosion Resistance

Bing Wang,^a Yingde Wang,^{*a} Yongpeng Lei,^{*b,d} Nan Wu,^a Yanzi gou,^a Cheng Han^a and Dong Fang^c

^aScience and Technology on Advanced Ceramic Fibres and Composites Laboratory, National University of Defense Technology, 109 Deya Road, Changsha 410073, PR China. Fax: 86 73184575118; Tel: 86 731 84575118; E-mail: wyd502@163.com

^bCollege of Basic Education, National University of Defense Technology, Changsha 410073, PR China; E-mail: lypkd@163.com

^cCollege of Materials Science and Engineering, Wuhan Textile University, Wuhan 430074, PR China

^dState Key Laboratory of Materials-Oriented Chemical Engineering, Nanjing University of Technology, Nanjing 210009, PR China.

Table and Figures for Electronic Supplementary Information

Table S1 The theoretical simulation results from *pseudo*-first-order and *pseudo*-second-order reaction model.

Label	<i>pseudo</i> -first-order model		<i>pseudo</i> -second-order model			
	$K_1 (\times 10^{-3} s^{-1})$	R^2	q_{e-exp}	q_{e-cal}	$K_2 (\times 10^{-3} g mg^{-1} s^{-1})$	R^2
MM-SFs	4.75	0.8046	19.52	19.12	10.44	0.9996
MMM-SFs	8.50	0.6782	19.98	20.04	13.74	0.9998

The initial MB concentration is 20 mg L⁻¹.

The correlation coefficients (R^2) value of both MM-SFs and MMM-SFs are greater than 0.999, revealing the kinetics of MB adsorption on the MM-SFs and MMM-SFs can be well described by the *pseudo*-second-order kinetic model. The experimental adsorption capacity (q_{e-exp}) values are close to the theoretical calculated adsorption capacity (q_{e-cal}) values resulted from pseudo-second order model. The larger K_1 and K_2 values of MMM-SFs present the faster adsorption rate.

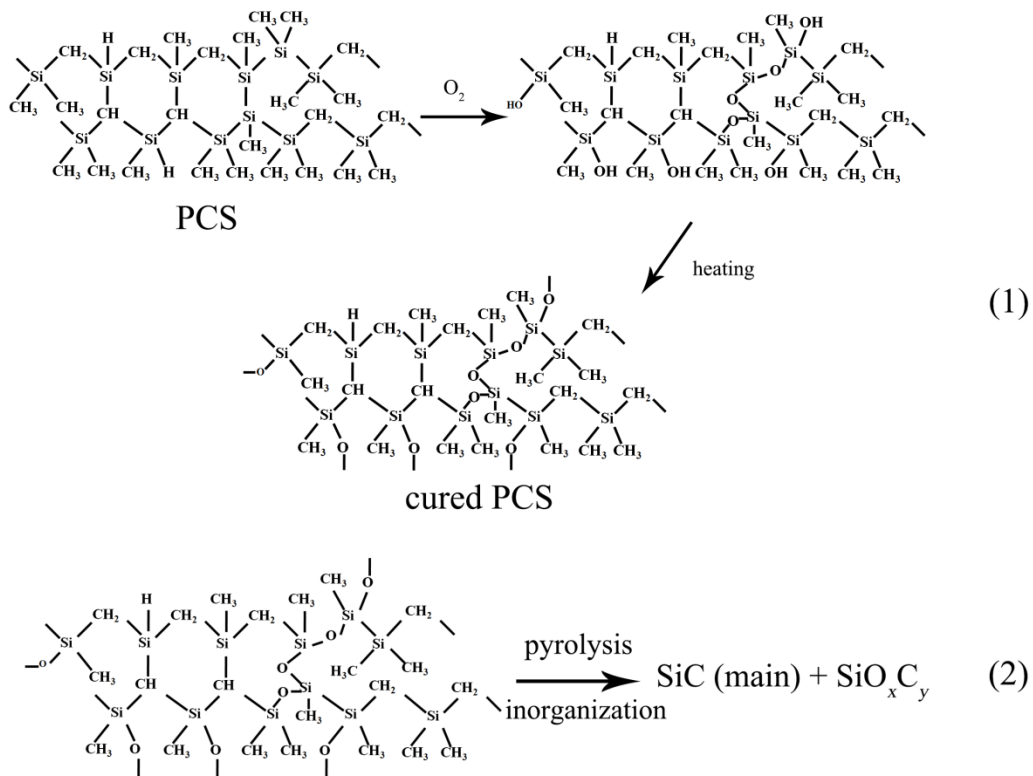


Fig. S1. The main chemical reaction occurred during the (1) air-curing process and (2) pyrolysis process. (References: Y. Hasegawa, *J. Mater. Sci.*, 1989, **24**, 1177.)

The air-curing process is carried out to prevent the fibers from merging together and keep the fibers' shape during the pyrolysis process and obtained high-strength SiC fibers. The structures of the resultant SiC fibers affected by the pyrolysis temperature has been detailedly discussed in the manuscript.

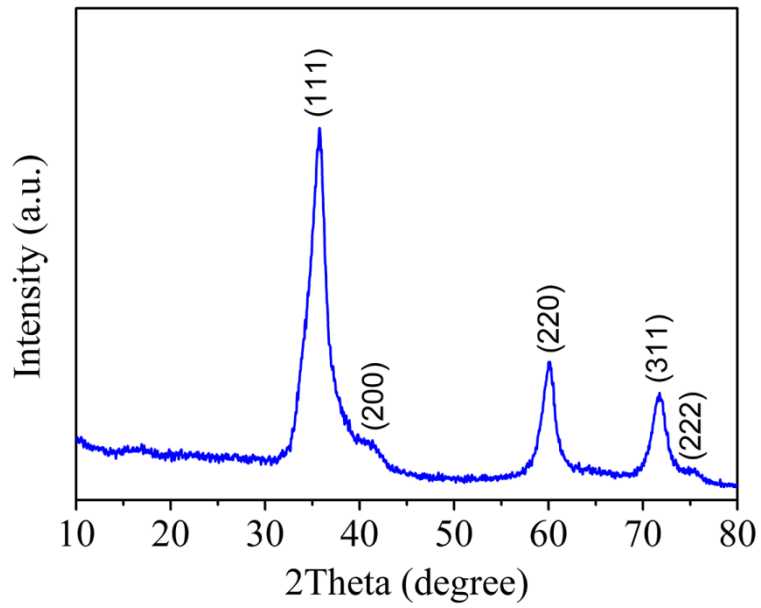


Fig. S2. The XRD pattern of the pristine SiC fibers. Compared with the XRD pattern of the MMM-SFs, there are no significant peaks shifts or phase structure change except that more stacking faults ($2\theta = 33.6^\circ$) were formed in MMM-SFs, which may be ascribed to the rich porous structure.

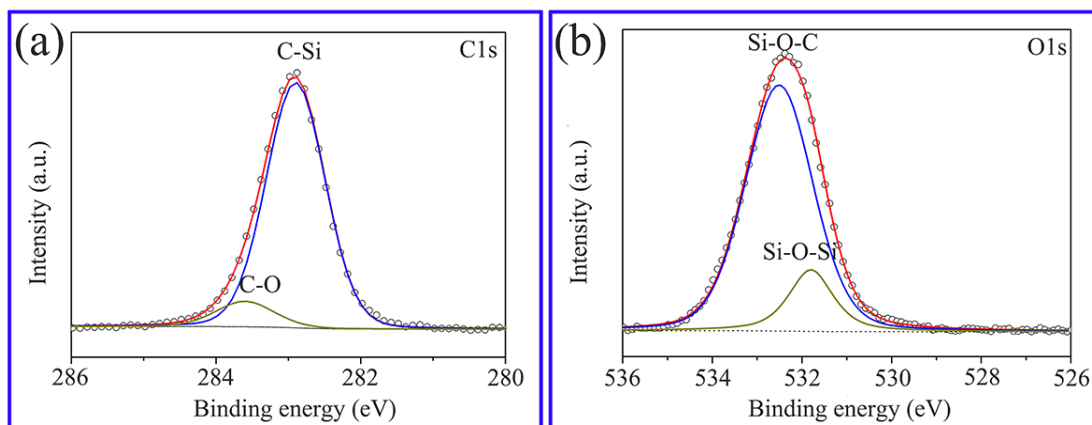


Fig. S3. The fitted XPS spectra of (a) C1s and (b) O1s of MMM-SFs, implying the main phase of SiC and the existence of SiC_xO_y phase.

The detailed C1s spectrum (Fig.S1a) conforms that Si-C bond at 282.9 eV is the main composition of MMM-SFs. And it demonstrates the existence of primarily C-O bond owing to the binding energy at 283.6 eV. The strongest peak at 532.3 eV corresponding to O 1s can be separated into two peaks at 531.8 eV and 532.5 eV, assigning to be the typical binding energy of a Si-O-C bond and Si-O-Si bond, respectively.

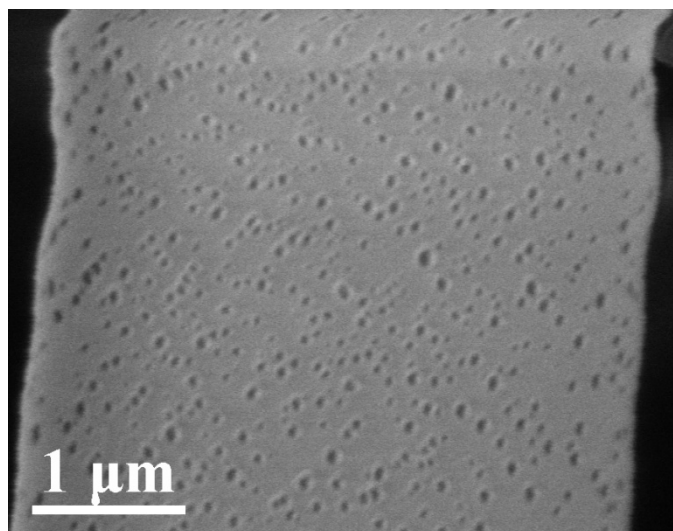


Fig. S4 The SEM image of macroporous PCS fibers, revealing the macropores were formed during electrospinning but not in the followed thermal-treated processes.

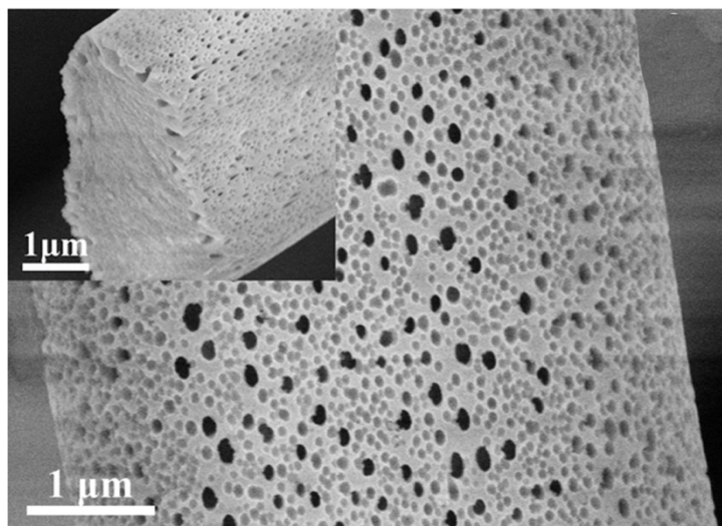


Fig. S5 The SEM images of MMM-SFs after adsorption for 5 cycles and calcined at 500 °C for 2h. The insets are the cross-section features. The pore structure was intact not only on the surface but in the core of the fibers.

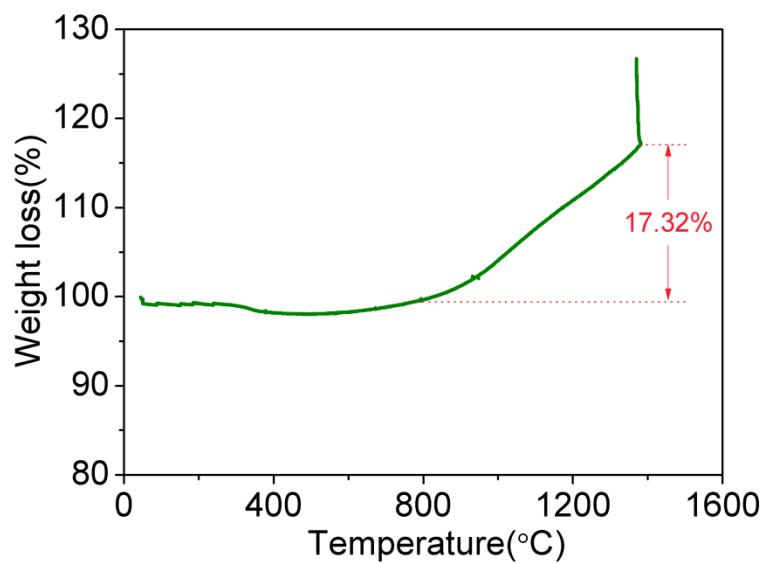


Fig. S6 The typical TGA analysis of MMM-SFs: heating from room temperature to 1400 °C and holding for 2h with ramping rate of 10 °C min⁻¹ under flow-air atmosphere. There is no weight raise occurred at the temperature below 800 °C and only 17.32 wt% weight gain happened from 800 to 1400 °C, indicating the outstanding thermal stability of the MMM-SFs.